

Davide Vito Moretti

Istituto di Ricovero e Cura a Carattere Scientifico  
(IRCCS) San Giovanni di Dio Fatebenefratelli,  
Brescia, Italy

Received 02 October 2014  
accepted 01 December 2014

# UNDERSTANDING EARLY DEMENTIA: EEG, MRI, SPECT AND MEMORY EVALUATION

## Abstract

**Background:** An increase in the EEG upper/low  $\alpha$  power ratio has been associated with mild cognitive impairment (MCI) due to Alzheimer's disease (AD) and to the atrophy of temporoparietal brain areas. Subjects with a higher  $\alpha3/\alpha2$  frequency power ratio showed lower brain perfusion than in the low  $\alpha3/\alpha2$  group. The two groups show significantly different hippocampal volumes and correlation with  $\theta$  frequency activity. **Methods:** Seventy-four adult subjects with MCI underwent clinical and neuropsychological evaluation, electroencephalogram (EEG) recording, and high resolution 3D magnetic resonance imaging (MRI). Twenty-seven of them underwent EEG recording and perfusion single-photon emission computed tomography (SPECT) evaluation. The  $\alpha3/\alpha2$  power ratio and cortical thickness were computed for each subject. The difference in cortical thickness between the groups was estimated. **Results:** In the higher upper/low  $\alpha$  group, memory impairment was more pronounced in both the MRI group and the SPECT MCI groups. An increase in the production of  $\theta$  oscillations was associated with greater interhemispheric coupling between temporal areas. It also correlated with greater cortical atrophy and lower perfusional rate in the temporoparietal cortex. **Conclusion:** High EEG upper/low  $\alpha$  power ratio was associated with cortical thinning and lower perfusion in temporoparietal areas. Moreover, both atrophy and lower perfusion rate significantly correlated with memory impairment in MCI subjects. Therefore, the increase in the EEG upper/low  $\alpha$  frequency power ratio could be useful in identifying individuals at risk for progression to AD dementia in a clinical context.

## Keywords

EEG • MRI • SPECT • Memory • Prodromal Alzheimer's disease


## Introduction

Mild cognitive impairment (MCI) commonly represents an "at-risk" state for the development of dementia. Therefore, there is a need for the development of early biomarkers which would help to identify subjects who could develop the disease and are useful for early diagnosis and effective prevention therapies. The identification and validation of biomarkers for diagnosing, monitoring progression, and predicting onset of Alzheimer's disease (AD) has been a main focus of AD research in the past 10 years. In line with recently published research criteria, it is becoming clear that the integration of different biomarkers is a milestone for the accurate and early diagnosis of AD [1,2]. To date, the most studied and validated biomarkers are  $A\beta_{1-42}$  and tau protein in the cerebrospinal fluid (CSF), glucose hypometabolism as determined by using fluorodeoxyglucose positron emission tomography ( $^{18}F$ -FDG PET), atrophy of hippocampal volume (HV) on magnetic resonance imaging (MRI), and brain amyloid deposition on amyloid imaging with PET [3,4].

The latter biomarkers have good sensitivity in identifying subjects with neurodegenerative disorders at high risk for converting to dementia, but they lack a reliable specificity that allows for a clear-cut diagnosis of the different subtypes of dementias. Of note, in neurodegenerative disorders like AD or other dementias, the brain networks are altered many years before clinical manifestations. Recent MRI studies have demonstrated that a large neural network is altered in subjects with prodromal AD [5-10]. In particular, subjects with cognitive decline have shown early atrophy and loss of grey matter in specific cortical brain areas, including precuneus, hippocampus, medial temporal, and parietal lobes [6,8]. EEG could be a reliable tool in the conceptual frame of the integration of biomarkers for an early and highly predictive diagnosis [11]. Indeed, it is widely accepted that cerebral EEG rhythms reflect the underlying brain network activity [12]. Furthermore, EEG coherence obtained from spectral EEG analysis is a non-invasive technique for studying functional and time-varying relationships between brain

regions. Indeed, EEG coherence represents the covariance of the spectral activity at two electrode locations and can be considered as a rough measure of the temporal synchronicity of coupled rhythmic oscillations of two distinct neural populations anatomically linked via corticocortical or corticosubcortical connections. In that sense, it reflects functional cortical coupling or connectivity [13]. As a consequence, modifications in EEG rhythms could be an early sign of AD. In particular, the study of  $\alpha$  rhythm seems to be a very suitable tool in detecting the relationship between structural and functional brain networks [14-17]. Recently, it has been demonstrated that an increase of the high  $\alpha$  relative to low  $\alpha$  power is a reliable EEG marker of hippocampal atrophy [18] and amygdalo-hippocampal complex atrophy [19]. Furthermore, an increase in the  $\alpha3/\alpha2$  power ratio has proven to be predictive of conversion of patients with MCI in AD, but not in non-AD dementia [20]. The same increase of the  $\alpha3/\alpha2$  power ratio was found to be correlated with hippocampal atrophy in subjects with AD [21-27] as well as with an

\* E-mail: [davide.moretti@afar.it](mailto:davide.moretti@afar.it)

 © 2015 Davide Vito Moretti, licensee De Gruyter Open.

This work is licensed under the Creative Commons Attribution-NonCommercial-NoDerivs 3.0 License.

increase in the functional interhemispheric coupling between temporoparietal areas [19]. On the other hand, subjects with a higher  $\alpha3/\alpha2$  frequency power ratio showed a constant trend towards lower perfusion than the low  $\alpha3/\alpha2$  group. The two groups differed significantly, both in regard to the hippocampal volume and correlation with the  $\theta$  frequency activity [27].

In this study, we observed an association between EEG coherence, MRI and single-photon emission computed tomography (SPECT) values, and memory impairment in the MCI group with a higher  $\alpha3/\alpha2$  frequency power ratio. Results show that in the higher upper/low  $\alpha$  group memory impairment was more pronounced in both the MRI group and the SPECT MCI group. Moreover, memory impairment in the higher upper/low  $\alpha$  group also correlated with greater cortical atrophy and lower perfusional value in the temporoparietal cortex along with an increase in functional coupling in the temporoparietal cortical areas.

## Materials and methods

### Subjects

Seventy-four subjects with MCI were recruited for the present study from The Memory Clinic of the Scientific Institute for Research and Care (IRCCS) of Alzheimer's disease (AD) and psychiatric diseases patients "Fatebenefratelli" in Brescia, Italy. All experimental protocols and appropriate procedures concerning human subjects were approved by the local Ethics

Committee. Informed consent was obtained from all participants or their caregivers according to the Code of Ethics of the World Medical Association (Declaration of Helsinki, Brasil, 2013).

### Diagnostic criteria

Patients were selected from a prospective study on the natural history of cognitive impairment (the translational outpatient memory clinic, TOMC study) carried out in the outpatient facility of the National Institute for the Research and Care of Alzheimer's Disease (IRCCS, Istituto Centro San Giovanni di Dio Fatebenefratelli, Brescia, Italy). Patients were rated with a series of standardized diagnostic and severity instruments, including the Mini-Mental State Examination (MMSE) [28], the Clinical Dementia Rating Scale (CDRS) [29], the Hachinski Ischemic Scale (HIS) [30], the Instrumental and Basic Activities of Daily Living (IADL, BADL) [31-33] and a complete neuropsychological assessment [34,35]. All the neuropsychological tests were standardized for the Italian population. The scores were compared to normative values with corrections for age, gender and educational level. In addition, patients underwent diagnostic neuroimaging procedures (MRI) and laboratory testing to rule out other causes of cognitive impairment. Inclusion criteria of the study were all of the following: (i) complaint by the patient, or report by a relative or the general practitioner, of memory or other cognitive disturbances; (ii)

MMSE score of 24-27/30, or MMSE of 28 and higher plus low performance (score of 2-6 or higher) on the clock drawing test [3]; (iii) sparing of IADL, BADL or functional impairment steadily due to causes other than cognitive impairment, such as physical impairments, sensory loss, gait or balance disturbances, etc. Exclusion criteria were any of the following: (i) patients aged 90 years and older (no minimum age to participate in the study); (ii) history of depression (from mild to moderate or major depression) or juvenile-onset psychosis; (iii) history or neurological signs of major stroke; (iv) other psychiatric diseases, overt dementia, epilepsy, drug addiction, alcohol dependence; (v) use of psychoactive drugs, including acetylcholinesterase inhibitors or other drugs enhancing brain cognitive functions or biasing EEG activity; and (vi) current or previous uncontrolled or complicated systemic diseases (including diabetes mellitus), or traumatic brain injuries. All subjects were right-handed. These inclusion and exclusion criteria for MCI were based on previous seminal studies [1,32,33]. As the aim of our study was to evaluate the relationship between gray matter loss and  $\alpha3/\alpha2$  ratios in MCI subjects, we did not consider the clinical subtype of MCI, i.e., amnesic, or non-amnesic, single or multiple domains. Demographic and cognitive features of the subjects in the study are summarized in Table 1. There were no statistical differences in age, gender, or education among the groups studied.

Table 1. Demographic and cognitive characteristics of the whole sample, disaggregated for increased levels of  $\alpha3/\alpha2$  numbers denote mean  $\pm$  standard deviation, number and [range]. p denotes significance on ANOVA.

	$\alpha3/\alpha2$			p
	High	Middle	Low	
<b>Demographic and clinical features</b>				
Number of subjects	18	38	18	
Age, years	70.4 $\pm$ 6.7 [60 - 85]	68.4 $\pm$ 8.2 [52 - 83]	70.4 $\pm$ 7.4 [57 - 80]	0.55
Sex, female	13 (%)	24 (%)	14 (%)	0.51
Education, years	6.6 $\pm$ 3.6 [4 - 18]	7.6 $\pm$ 3.7 [3 - 17]	8.3 $\pm$ 4.7 [3 - 18]	0.42
Mini-Mental State Examination	27 $\pm$ 1.7 [23 - 29]	27.4 $\pm$ 1.3 [24 - 30]	26.9 $\pm$ 1.2 [23 - 30]	0.46
WMHs (mm <sup>3</sup> )	2.78 $\pm$ 2.58	5.59 $\pm$ 6.60	2.57 $\pm$ 2.76	0.09
$\alpha3/\alpha2$	1.29 $\pm$ 0.1 [1.17 - 1.52]	1.08 $\pm$ 0.0 [1 - 1.16]	0.9 $\pm$ 0.1 [0.77 - 0.98]	0.000

## EEG recordings

The EEG activity was recorded continuously from 19 sites by using electrodes set in an elastic cap (Electro-Cap International, Inc., Eaton, OH, USA) and positioned according to the 10-20 international system (Fp1, Fp2, F7, F3, Fz, F4, F8, T3, C3, Cz, C4, T4, T5, P3, Pz, P4, T6, O1, and O2). The patients were instructed to stay seated with their eyes closed and relaxed. In order to keep constant the level of vigilance, an operator controlled the subject and the EEG traces on-line, alerting the subject any time there were signs of behavioral and/or EEG drowsiness. The ground electrode was placed in front of Fz. The left and right mastoids served as reference for all electrodes. The recordings were used off-line to re-reference the scalp recordings to the common average. Re-referencing was done prior to the EEG artifact detection and analysis. Data were recorded with a band-pass filter of 0.3-70 Hz, and digitized at a sampling rate of 250 Hz (BrainAmp, BrainProducts GmbH, Munich, Germany). Electrode-skin impedance was set below 5 k $\Omega$ . Horizontal and vertical eye movements were detected by recording the electrooculogram (EOG). The recording lasted 5 min, with the subjects' eyes closed. Longer recordings would have reduced the variability of the data, but they would also have increased the possibility of the slowing of EEG oscillations due to reduced vigilance and arousal. EEG data were then analyzed and fragmented off-line in consecutive epochs of 2 s, with a frequency resolution of 0.5 Hz. We are confident about the stationarity of the EEG signal in our traces. Our recordings were performed at rest state, without any external stimulation that could bias the signal, maintaining the stochastic nature of spontaneous ongoing EEG. Moreover, although it is widely accepted that the duration of a so-called quasi-stationary interval of continuous EEG recordings is expected not to exceed 2-4 s [36], some authors found much longer fragments of even 12 s [37], 25 s [38] or 40-60 s [39] to be approximately stationary. Of note, our spectral analysis has been evaluated on two-second epochs in each subject. Finally, the spectral power was averaged across all electrodes to obtain a sort of global field

power, which would have reduced the channel to channel variability, with the advantage of extracting a high stationary measure and obtaining a smoother, clearer and more homogeneous individual  $\alpha$  peak. Recently it has been demonstrated that the analysis of the EEG recording in frequency domain (i.e. power spectra) results in high stationary signal [40]. As a control analysis, the stability of the EEG signal was tested as follows: the power spectra of ten epochs lasting two seconds each were averaged both at the beginning and at the end of the artifact-free EEG trace of all subjects, since testing for stationarity of the variability of trial-to-trial power spectra required equal time intervals between consecutive observations [40]. Analyses of variance (ANOVA) showed no statistical difference ( $p = 0.2$ ) between the beginning and the ending epochs in each subject and among all subjects. The average number of epochs analyzed was 140, ranging from 130 to 150. The epochs with ocular, muscular, and other types of artifacts were discarded by two skilled electroencephalographers [17]. The spectral power obtained was an estimation of a spectrum collapsed all over the scalp electrodes. In this way, the eventual contribution of the muscular artifact was strongly reduced. It should have been possible to compute a more focused field, choosing a subset of electrodes next to the brain region of interest. However, this procedure has two main disadvantages: 1) it needs a larger array of electrodes, given the volume conduction phenomenon. Of note, a larger electrode array should require the application of some further computation, e.g. Laplacian filter or spline interpolation; this aspect is of particular importance because it is more time-consuming and is not applicable in a clinical context; 2) the power computation on a smaller number of electrodes could give rise to artifactual detection of the individual  $\alpha$  frequency peak as the presence of double peak or the absence of a clear peak. These computation errors are overlooked by the power spectra computation collapsed on the whole array of electrodes. Moreover, two skilled electroencephalographers checked the data individually and then held a mutual

revision session afterward. No automatic methods were used. We are confident that this control procedure can prevent the insertion of artifactual EEG segments into the analysis.

## Analysis of individual frequency bands

All recordings were obtained in the morning with subjects resting comfortably. Vigilance was continuously monitored in order to avoid drowsiness. A digital fast Fourier transform (FFT)-based power spectrum analysis (Welch technique, Hanning windowing function, no phase shift) computed the power density of EEG rhythms ranging from 2 to 45 Hz with a 0.5 Hz frequency resolution. Two anchor frequencies were selected according to the literature guidelines [17,20], that is, the  $\theta/\alpha$  transition frequency (TF) and the individual  $\alpha$  frequency (IAF) peak. IAF and TF were computed for each subject in the study. These anchor frequencies were computed on the power spectra averaged across all recording electrodes. This "collapsed spectrum method" allows for identification of a robust and reliable IAF, being a normalized scalp spectrum. Finally, given that we were interested in the resting state spectral content, the  $\alpha$  band and IAF were determined during the "eyes closed" period. There is a large body of literature showing that the standard frequency range found in young and healthy people is not applicable in healthy older people and patients affected by brain degenerative disorders due to the effect of both age and disease [41-46]. As a consequence, the computation of an individual  $\alpha$  frequency peak is mandatory in our study. Recent studies have convincingly shown that the IAF is very reliable in rest condition EEG recording [47-49]. More caution has been suggested when the study requires subjects to perform some specific tasks [50]. The TF marks the transition frequency between  $\theta$  and  $\alpha$  bands, and represents an estimate of the frequency at which  $\theta$  and  $\alpha$  spectra intersect. TF was computed as the minimum power in the  $\alpha$  frequency range, since our EEG recordings were performed at rest. The IAF represents the frequency with the maximum power peak within the extended  $\alpha$  range (5-14 Hz). Based on TF and IAF, we estimated the frequency band range for each subject, as

follows:  $\delta$  from TF-4 to TF-2,  $\theta$  from TF-2 to TF, low  $\alpha$  band ( $\alpha_1$  and  $\alpha_2$ ) from TF to IAF, and high  $\alpha$  band (or  $\alpha_3$ ) from IAF to IAF +2. The  $\alpha_1$  and  $\alpha_2$  bands were computed for each subject as follows:  $\alpha_1$  from TF to the middle point of the TF-IAF range, and  $\alpha_2$  from such middle point to the IAF peak. Moreover, individual  $\beta$  and  $\gamma$  frequencies were computed. Three frequency peaks were detected in the frequency range from the individual  $\alpha_3$  frequency band to 45 Hz. These peaks were named  $\beta_1$  peak (IBF1),  $\beta_2$  peak (IBF2) and  $\gamma$  peak (IGF). Based on peaks, the frequency ranges were determined.  $\beta_1$  ranges from  $\alpha_3$  to the lower spectral power value between  $\beta_1$  and  $\beta_2$  peak;  $\beta_2$  frequency ranges from  $\beta_1$  to the lower spectral power value between  $\beta_2$  and  $\gamma$  peak;  $\gamma$  frequency ranges from  $\beta_2$  to 45 Hz, which is the end of the range considered. Moreover, within theta ( $\theta$ ) frequency the frequency peak (individual  $\theta$  frequency, ITF) was also individuated. The mean frequency ranges computed in MCI subjects considered as a whole were:  $\delta$  2.9-4.9 Hz;  $\theta$  4.9-6.9 Hz;  $\alpha_1$  6.9-8.9 Hz;  $\alpha_2$  8.9-10.9 Hz;  $\alpha_3$  10.9-12.9 Hz;  $\beta_1$  12.9-19.2 Hz;  $\beta_2$  19.2-32.4;  $\gamma$  32.4-45. Finally, in the frequency bands determined on an individual basis, we computed the relative power spectra for each subject. The relative power density for each frequency band was computed as the ratio between the absolute power and the mean power spectra from 2 to 45 Hz. The relative band power at each band was defined as the mean of the relative band power for each frequency bin within that band. The  $\alpha_3/\alpha_2$  was computed in all subjects and three groups were obtained according to increasing tertile values of  $\alpha_3/\alpha_2$ : low ( $\alpha_3/\alpha_2 < 1$ ), middle ( $1 < \alpha_3/\alpha_2 < 1.16$ ) and high ( $\alpha_3/\alpha_2 > 1.17$ ). The tertile division allows a balanced distribution of the study samples with the advantage of avoiding extreme values in the statistical analysis. The three groups of MCI have, in previous studies, been shown to be different in nature. In particular, the high  $\alpha_3/\alpha_2$  EEG power ratio MCI group is at major risk for converting to AD [19], as well as for having a different pattern of hippocampal atrophy [20] and basal ganglia and thalamus gray matter lesions [22], as compared to the other  $\alpha_3/\alpha_2$  power ratio MCI groups. Moreover, this group subdivision has been chosen for the reason

of homogeneity and comparability with the previous studies.

### EEG spectral coherence

EEG coherence represents the covariance of the EEG spectral activity at two electrode locations and can be considered as a measure of temporal synchronization of the EEG signals recorded at pairs of electrodes. These signals mainly reflect the oscillatory dendrite activity of the cortical pyramidal neurons, so ideally the coherence estimates represent the temporal synchronization or functional coupling of the two cortical populations generating the scalp EEG data collected by the paired electrodes. In reality, the coherence estimates are affected by currents that are volume-conducted by remote EEG sources. Furthermore, these estimates are typically not zero in the case of absent coupling; actually the value depends upon the number of epochs used in the computation. Finally, coherence analysis just captures the linear component of the functional coupling of the paired EEG oscillations when compared with modern nonlinear approaches. However, despite the mentioned limitations, the coherence analysis of EEG data is a basic tool available in practically all digital EEG machines used for clinical applications. This is why the analysis of EEG coherence is the most common methodological approach for the study of functional coupling of EEG oscillations in aging. Here, coherence was calculated by the following equation:

$$\text{Coh}_{xy}(\lambda) = \frac{|R_{xy}(\lambda)|^2}{f_{xx}(\lambda) f_{yy}(\lambda)}$$

where  $f$  denotes the spectral estimate of two EEG signals  $x$  and  $y$  for a given frequency bin ( $\lambda$ ). The numerator contains the cross-spectrum for  $x$  and  $y$  ( $f_{xy}$ ), while the denominator contains the respective autospectra for  $x$  ( $f_{xx}$ ) and  $y$  ( $f_{yy}$ ). This procedure returns a real number between 0 (no coherence) and 1 (max coherence). The EEG coherence was computed at the frontotemporal (F3-T and F4-T4), temporoparietal (T3-P3 and T4-P4) and frontoparietal electrode pairs of interest (F3-P3, F4-P4) to obtain intrahemispheric coherence. Furthermore, EEG coherence was computed at frontal, temporal and parietal electrode pairs

of interest (F3-F4, T3-T4 and P3-P4) to obtain interhemispheric coherence. Coherence was computed both in normal controls and in MCI subjects.

### MRI scans

For each subject, a high-resolution sagittal T1 weighted volumetric MRI scan was acquired at the Neuroradiology Unit of the "Città di Brescia" Hospital, Brescia, Italy, by using a 1.0 T Philips Gyroscan scanner (Philips Medical Systems, Best, The Netherlands), with a gradient echo 3D technique: TR = 20 ms, TE = 5 ms, flip angle = 30, field of view = 220 mm, acquisition matrix 256 · 256, slice thickness 1.3 mm.

### Cortical thickness estimation steps

Cortical thickness measurements for 74 MCI patients were made using a fully automated MRI-based analysis technique: FreeSurfer v5.1.0 (www.freesurfer.net), a set of software tools for the study of cortical and subcortical anatomy. Briefly, in the cortical surface stream, the models of the boundary between white matter and cortical gray matter as well as the pial surface were constructed [51]. Once these surfaces are known, an array of anatomical measures becomes possible, including: cortical thickness, surface area, curvature, and surface normal at each point on the cortex [52]. In addition, a cortical surface-based atlas has been defined based on average folding patterns mapped to a sphere and surfaces from individuals can be aligned with this atlas with a high-dimensional non-linear registration algorithm. The surface-based pipeline consists of several stages previously described in detail [53,54].

### Single subject analysis

For each subject the T1-weighted, anatomical 3-D MRI dataset were converted from DICOM format into .mgz format, then intensity variations were corrected and a normalized intensity image created. The volume was registered with the Talairach-Tournoux atlas through an affine registration. Next, the skull was stripped using a deformable template model [52] and extracerebral voxels removed. The intensity normalized, skull-stripped image was then operated on by a segmentation procedure based on the geometric structure of

the gray-white interface. Voxels were classified as white or grey matter, cutting planes were chosen to separate the hemispheres from each other. A white matter surface was then generated for each hemisphere by tiling the outside of the white matter mass for that hemisphere. This initial surface was then refined to follow the intensity gradients between the white and gray matter. The white surface was then nudged to follow the intensity gradients between the gray matter and CSF, obtaining the pial surface. Cortical thickness measurements were obtained by calculating the distance between those surfaces (white and pial surface) at each of approximately 160,000 points per hemisphere across the cortical mantle [53-59].

### Group analysis

In order to relate and compare anatomical features across subjects, it is necessary to establish a mapping that specifies a unique correspondence between each location in one brain and the corresponding location in another. Thus, the pial surface of an individual subject was inflated to determine the large-scale folding patterns of the cortex and subsequently transformed into a sphere to minimize metric distortion. The folding patterns of the individual were then aligned with an average folding pattern using a high-resolution surface-based averaging. Thickness measures were mapped to the inflated surface of each participant's brain reconstruction allowing visualization of data across the entire cortical surface. Finally, cortical thickness was smoothed with a 20-mm full width at half height Gaussian kernel to reduce local variations in the measurements for further analysis.

### SPECT scan

Twenty-seven patients and 17 normal controls underwent SPECT scan in the nuclear medicine department of the Ospedali Riuniti hospital, Bergamo, Italy. Each subject received an intravenous injection of 925 MBq of technetium-99m-L,L-ethyl cysteinate dimer ( $^{99m}\text{Tc}$ -ECD) in resting conditions, lying supine with closed eyes in a quiet, dimly lit room. Forty to sixty minutes after injection, brain SPECT was performed using a dual-head rotating  $\gamma$  camera (GE Elscint Helix, General Electric Healthcare, Little

Chalfont, UK) equipped with low-energy, high-resolution parallel hole collimators. A 128 x 128 pixel matrix, zoom = 1.5, was used for image acquisition with 120 views over a 360° orbit (in 3° steps) with a pixel size and slice thickness of 2.94 mm. Butterworth filtered-back projection (order = 7, cutoff = 0.45 cycles/cm) was used for image reconstruction, and attenuation correction was performed using Chang's method (attenuation coefficient = 0.11/cm). Images were exported in DICOM format.

### SPECT processing protocol

To achieve a precise normalization, we generated a study-specific SPECT template using both SPECT and MRI scans of all patients and normal controls under study, following a procedure described in detail elsewhere [60]. Briefly, we created a customized high-definition MRI template, converted SPECT scans to Analyze format using MRIcro and coregistered them to their respective MRI scans with SPM2 (SPM, Statistical Parametric Mapping, version 2, Functional Imaging Laboratory, London, UK). We normalized each MRI to the customized MRI template through a nonlinear transformation (cutoff 25 mm), and applied the normalization parameters to the co-registered SPECT. We obtained the customized SPECT template as the mean of all the latter normalized SPECT images. The creation of a study-specific template allows for better normalization, since low uptake in ventricular structures and the cortical hypoperfusion effects are frequently present in elderly patients. For each coregistered SPECT scan, we set origin to the anterior commissure, using the respective MRI image as a reference, and we processed all scans with SPM2 according to an optimized processing protocol described in detail elsewhere [60]. Brain perfusion correlates of medial temporal lobe atrophy and white matter hyperintensities in MCI were obtained as follows: (I) we smoothed each scan with a 10 mm full width at half maximum (FWHM) Gaussian, and spatially normalized it with an affine deformation to the customized SPECT template. We applied the same deformation to the non-smoothed images; (II) we masked the non-smoothed normalized images from I to remove scalp activity using SPM2's "brainmask". We smoothed with a 10 mm FWHM Gaussian,

and warped them to the customized template with a nonlinear transformation (cutoff 25 mm). We applied the same transformation to the non-smoothed masked images; (III) we smoothed the normalized non-smoothed images from II with a 12 mm FWHM Gaussian. The following Regions of Interest (ROI) were chosen for perfusion analyses in each hemisphere from the Pick atlas by a subroutine implemented on SPM2: frontal, parietal and temporal lobes, the thalamus and the amygdalo-hippocampal complex [60].

### MRI statistical analysis

Differences between groups in sociodemographic and neuropsychological features were analyzed using SPSS version 13.0 (SPSS, Chicago, IL, USA) performing an analysis of variance (ANOVA) for continuous variables and paired  $\chi^2$  test for dichotomous variables. For continuous variables, *post-hoc* pairwise comparisons among groups were performed with the Games-Howell or Bonferroni tests, depending on homogeneity of variance tested with Levene's test.

Concerning the neuroimaging analysis, the Qdec interface in Freesurfer software was used: a vertex-by-vertex analysis was carried out performing a general linear model to analyse whether any difference in mean cortical thickness existed between groups (low:  $\alpha_3/\alpha_2 < 1 \mu\text{V}^2$ ; middle:  $1 < \alpha_3/\alpha_2 < 1.16 \mu\text{V}^2$ ; high:  $\alpha_3/\alpha_2 > 1.17 \mu\text{V}^2$ ). The following comparisons were carried out: high versus low, high vs middle and middle vs low. Age, sex, education, global cognitive level (MMSE score) and white matter hyperintensities (WMHs) were introduced as covariates in the analysis to avoid confounding factors. We first tried to apply an appropriate Bonferroni multiple-comparison correction in our analysis (at  $p < 0.05$  corrected). Unfortunately, no  $p$ -value survived after this correction. Thus we choose to set a more restrictive significance threshold (than  $p < 0.05$  corrected) at  $p < 0.001$  uncorrected for multiple comparisons. Moreover, we considered as significant only the clusters which were also wide equal or greater than 30 mm<sup>2</sup>. Finally, a surface map was generated to display the results on an average brain. For illustrative purposes, significance was set to a  $p$ -value of  $< 0.01$  uncorrected for multiple comparisons.



### Memory tests statistical analysis

As a control analysis, in order to exclude casual relationships between EEG markers and cortical volumes, a correlation between brain areas and memory performance has been studied. The correlation analysis was performed on the three samples separately (high  $\alpha3/\alpha2$ , low  $\alpha3/\alpha2$ , middle  $\alpha3/\alpha2$ ) and on the entire sample (high, low, and middle grouped together). An exploratory analysis of non-linear correlation did not fit into the purpose of testing our *a priori* hypothesis. We chose to apply a measure of linear dependence led by our *a priori* hypothesis for which the MCI group with the greater cortical thinning and higher  $\alpha3/\alpha2$  EEG level (indicating an incipient AD) should show a clear correlation with the memory tests performance, in the sense that an increase in cortical thinning corresponds to a decrease in memory performance, and vice versa. Indeed, even if in the cognitive tests scores there could have been no significant differences, we hypothesized that the MCI group with the greater cortical thinning and higher  $\alpha3/\alpha2$  EEG level, indicating an incipient AD, should show a clear correlation with memory test performance. The correlation analysis on a vertex-by-vertex basis was performed specifically for the following neuropsychological memory test results: Babcock Test, Rey auditory verbal learning test (AVLT) immediate recall, and Rey AVLT delayed recall. The analysis was thresholded at  $p < 0.001$  uncorrected for multiple comparisons while results were mapped at  $p$ -value of less than 0.005 uncorrected for illustrative purposes. Only the clusters which survived at the statistical threshold and were wide equal or greater than 15 mm<sup>2</sup> were considered significant.

### EEG coherence statistical analysis

The EEG coherence session was composed of three ANOVAs for 1) left and 2) right intrahemispheric and 3) interhemispheric coherence. Each ANOVA was a 3-way interaction with group as independent variable, and electrode pairs and frequency as dependent variables. The Greenhouse-Geisser correction and Mauchly's sphericity test were applied to all ANOVAs.

### SPECT statistical analysis

All statistical analyses were performed using SPSS software ver. 13.0. We investigated the significance of the difference between the two groups (MCI at low and at high risk to developing AD) in socio-demographic, clinical, and cognitive features using  $\chi^2$  test for categorical variables (sex, and ApoE) and Student's independent t test for continuous variables (volumetric, perfusion features and EEG frequencies). In all cases we set the significance threshold of  $p < 0.05$ . Since native SPECT scans were co-registered to their respective MRI images, and the study-specific SPECT template was co-registered to the high-definition MRI template, all the normalized SPECT and MRI images used for the statistical analysis were co-registered to the SPM standard anatomical space. Moreover, Pearson's r correlations were assessed between the selected perfusion ROIs (in terms of age-corrected W scores) and the acquired EEG frequencies in both groups.

## Results

### a) MRI

Table 1 shows the sociodemographic and neuropsychological characteristics of MCI subgroups defined by the tertile values of  $\alpha3/\alpha2$ . The ANOVA analysis showed that there were

no statistically significant differences between groups in regard to age, sex, WMHs burden, education, and global cognitive level. Age, sex, education, global cognitive level (MMSE score), and WMHs were introduced as covariates in the subsequent analysis to avoid confounding factors.  $\alpha3/\alpha2$  ratio levels were significant at Games-Howell *post hoc* comparisons ( $p = 0.000$ ). The data of the same subjects were used in previously published works of our group [41-43].

### Pattern of cortical thickness between groups

High vs low: When compared to subjects with low  $\alpha3/\alpha2$  ratios, patients with high  $\alpha3/\alpha2$  ratio showed thinning in the bilateral superior temporal, supramarginal and precuneus cortices, as well as in the right inferior parietal cortex and insula. The total cortical gray matter (CGM) reduction in high  $\alpha3/\alpha2$  group vs low  $\alpha3/\alpha2$  group was 471 mm<sup>2</sup> (Fig. 1).

High vs middle: The same (high) group showed a similar but less wide pattern of cortical thinning when compared to middle  $\alpha3/\alpha2$  group: the regions of atrophy were located in the left supramarginal gyrus, left precuneus and postcentral cortex. The total CGM reduction in high  $\alpha3/\alpha2$  group versus middle  $\alpha3/\alpha2$  group was 160 mm<sup>2</sup> (Fig. 2). When the high group was compared to the low

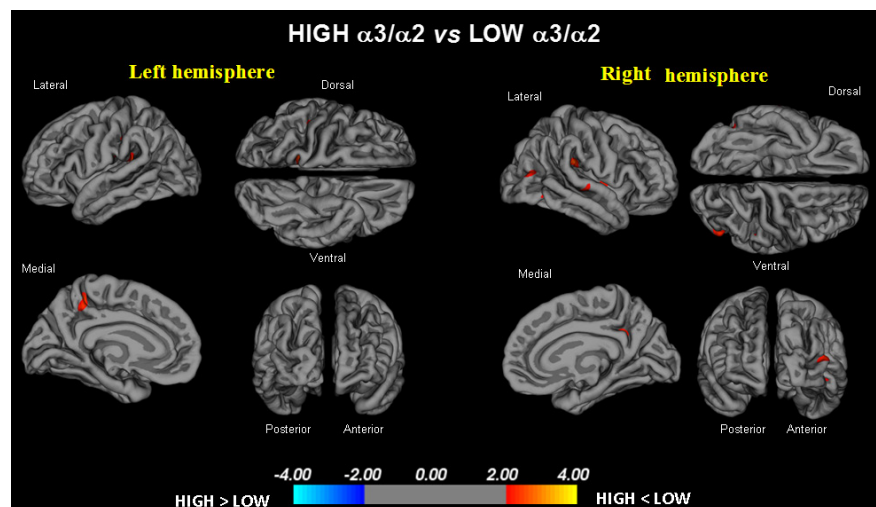


Figure 1. The brain regions with higher regional cortical thickness in MCI with a high  $\alpha3/\alpha2$  ratio as compared to MCI with low  $\alpha3/\alpha2$  ratio ( $p < 0.01$  uncorrected) are represented in red. The color-coding for  $p$  values is on a logarithmic scale. Results are presented on the pial cortical surface. Dark gray regions represent sulci and light gray regions represent gyri.

group the total extension of cortical thinning (471 mm<sup>2</sup>) was 34% wider than when the high group was compared to the middle group (160 mm<sup>2</sup>). No regions of major cortical atrophy were found in the groups with middle or low  $\alpha3/\alpha2$  power ratio when compared to the high  $\alpha3/\alpha2$  group. No significant cortical thickness differences were found between the middle and low  $\alpha3/\alpha2$  groups.

### EEG coherence results

The ANOVA results for right intrahemispheric coherence revealed significant interactions between groups, frequency, and electrode pairs ( $F_{14,1596} = 5.54$ ;  $p < 0.0000$ ). Duncan's *post-hoc* test showed a significant decrease in all frequencies on all electrode pairs (all  $P$ 's  $< 0.0001$ ) in the MCI group. Other comparisons were not significant.

The ANOVA results for interhemispheric coherence (Fig. 3) also revealed significant interactions between groups, frequency, and electrode pairs ( $F_{14,1596} = 2.27$ ;  $p < 0.0047$ ). Duncan's *post-hoc* test showed a significant increase in all frequencies ( $p < 0.05$ ) that were particularly significant in  $\theta$  frequency on temporoparietal electrodes (all  $p$ 's  $< 0.001$ ) in MCI group. Other comparisons were not significant.

The ANOVA results for the left intrahemispheric coherence revealed significant interactions between groups, frequencies, and electrode pairs ( $F_{14,1596} = 5.05$ ;  $p < 0.0000$ ). Duncan's *post-hoc* test showed a significant decrease in all frequencies on all electrode pairs (all  $p$ 's  $< 0.0001$ ) in the MCI group. Other comparisons were not significant.

### Correlations between neuropsychological memory tests and cortical thickness in the high $\alpha3/\alpha2$ group and the other groups

*Babcock test*: a significant positive correlation was found in the high  $\alpha3/\alpha2$  group between logical memory performance at Babcock test and thickness values in the left caudal middle frontal cortex (cluster size = 36 mm<sup>2</sup>; stereotaxic coordinate  $x, y, z = -34\ 22\ 47$ ;  $r = 0.80$ ;  $p = 0.0001$ ), left inferior temporal cortex (15 mm<sup>2</sup>;  $-54\ -28\ -26$ ;  $r = 0.72$ ;  $p = 0.001$ ), and right rostral middle frontal cortex (28 mm<sup>2</sup>;  $23\ 56\ -13$ ;  $r =$

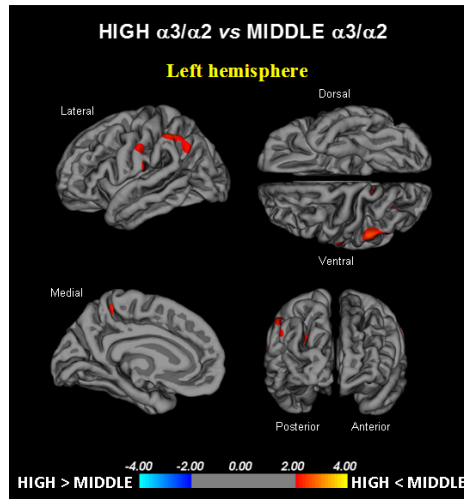


Figure 2. The brain regions with higher regional cortical thickness in MCI subjects with a high  $\alpha3/\alpha2$  ratio as compared to MCI subjects with a middle  $\alpha3/\alpha2$  ratio are represented in red ( $p < 0.01$  uncorrected). The color-coding for  $p$  values is on a logarithmic scale. Results are presented on the pial cortical surface. Dark gray regions represent sulci and light gray regions represent gyri.

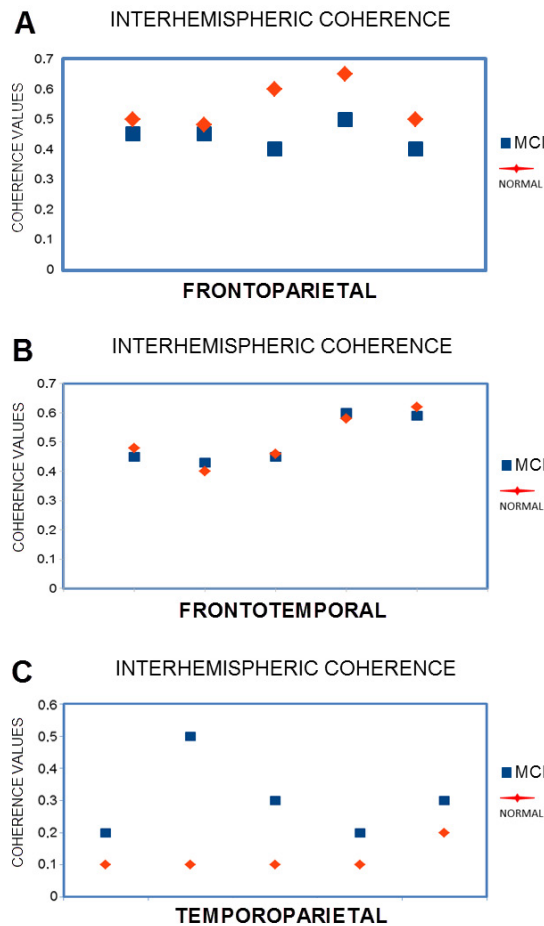


Figure 3. EEG coherence statistical results. A. frontoparietal interhemispheric coherence, B. frontotemporal interhemispheric coherence, C. temporoparietal interhemispheric coherence.

0.74;  $p = 0.0007$ ) (Fig. 2). No other significant correlations emerged in the same regions, in the other groups, or in the whole sample.

*AVLT immediate recall:* in the high  $\alpha3/\alpha2$  group, memory performance significantly correlated with the cortical thickness values in the bilateral precuneus (left: 47 mm<sup>2</sup>; -21 -61 20;  $r = 0.78$ ;  $p < 0.0000$ ; right: 58 mm<sup>2</sup>; 20 -60 25;  $r = 0.72$ ;  $p = 0.0007$ ), cortex of the left fusiform gyrus (40 mm<sup>2</sup>; -41 -25 -21;  $r = 0.76$ ;  $p = 0.0005$ ), inferior parietal (43 mm<sup>2</sup>; -46 -60 11;  $r = 0.74$ ;  $p = 0.0001$ ), inferior temporal cortex (35 mm<sup>2</sup>; -53 -34 -21;  $r = 0.71$ ;  $p = 0.0008$ ), and the right bank of the cortex in the superior temporal sulcus (44 mm<sup>2</sup>; 48 -48 9;  $r = 0.81$ ;  $p < 0.000$ ). Memory performance also correlated in the middle group with both the cortical thickness of the right precuneus ( $r = 0.19$  and  $p = 0.03$ ), and the right bank of the superior temporal sulcus ( $r = 0.44$ ,  $p = 0.02$ ). No significant associations were found neither in the low group nor the entire sample.

*AVLT delayed recall:* in the high  $\alpha3/\alpha2$  group, memory function correlated significantly with cortical thickness in the bilateral inferior parietal (left: 95; -44 -58 12;  $r = 0.86$ ;  $p < 0.0000$ ; right: 49; 50 -50 9;  $r = 0.74$ ;  $p = 0.0005$ ), left pericalcarine cortex (54; -7 -8 11;  $r = 0.76$ ;  $p < 0.0000$ ), bank of the superior temporal sulcus (31; -51 -41 -5;  $r = 0.81$ ;  $p = 0.0002$ ) and in the right superior temporal cortex (22; 56 -34 13;  $r =$

0.73;  $p = 0.001$ ). No other significant correlation was found between the same regions, in the other groups, or in the whole sample.

**b) SPECT**

Twenty-seven MCI patients were enrolled for the present study and were classified as being at high risk (when the  $\alpha3/\alpha2$  EEG rhythm median was above 1.17) or at low risk (when the  $\alpha3/\alpha2$  EEG rhythm median was under 1.17) for

developing AD. The two groups (AD high risk,  $N = 13$ , AD low risk,  $N = 14$ ) were similar for age ( $p = 0.56$ ), education in years ( $p = 0.87$ ), gender ( $p = 0.17$ ), ApoE genotype ( $p = 0.15$ ), MMSE scores ( $p = 0.31$ ) and white matter lesions load ( $p = 0.88$ ; Table 2). Figure 4 shows the visual rating scale of the SPECT scans representative of the normal control, MCI with low, and MCI with high risk to conversion to AD, respectively. ANOVA results show that

**Table 2.** Demographic and cognitive characteristics of the SPECT subjects sample, disaggregated for increased levels of  $\alpha3/\alpha2$ . Numbers denote mean  $\pm$  standard deviation, number and [range].  $p$  denotes significance on ANOVA.

	At low-risk MCI	At high-risk MCI	$p$
N	14	13	
Age (years) [range]	69.1 $\pm$ 7.6 [57 - 83]	70.6 $\pm$ 5.5 [62 - 78]	0.555
Gender (females)	6 (43%)	9 (69%)	0.168
Education (years) [range]	8.2 $\pm$ 4.3 [4 - 18]	7.9 $\pm$ 4.5 [3 - 18]	0.865
MMSE score [range]	27.9 $\pm$ 1.6 [25 - 30]	27.2 $\pm$ 1.9 [24 - 29]	0.309
ApoE $\epsilon 4$ genotype (carriers)	2 (29%)	5 (39%)	0.152
Left hippocampal volume (mm <sup>3</sup> ) [range]	2,606 $\pm$ 353 [1,923 - 3,017]	2,073 $\pm$ 412 [1,234 - 2,641]	0.001*
Right hippocampal volume (mm <sup>3</sup> ) [range]	2,581 $\pm$ 473 [1,549 - 3,150]	2,296 $\pm$ 501 [1,589 - 3,086]	0.141
Wahlund total score* [range]	3.58 $\pm$ 3.29 [0.0 - 10.0]	3.78 $\pm$ 2.63 [0.0 - 7.0]	0.886

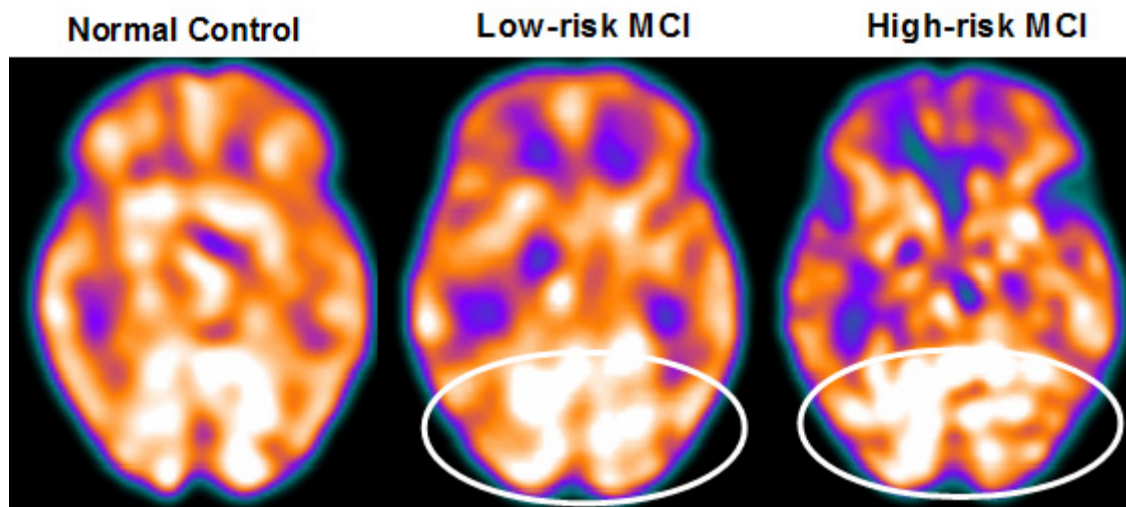


**Figure 4.** SPECT visual rating. The output shows a SPECT visual inspection of glucose uptake metabolism: the white ellipses denote an area of mild-to-moderate hypometabolism in one of the 14 at low risk and in one of the 13 at high risk MCI patients with respect to one of the 17 enrolled controls (unlabeled on the left side).



the selected cutoff was effective in detecting patients with high risk for developing AD, who show significantly higher  $\alpha3/\alpha2$  power ratio than patients with low risk ( $p = 0.0001$ ). Moreover, a control analysis was performed on the single frequencies. The results show that the increase of  $\alpha3/\alpha2$  frequency power ratio was due to both an increase in  $\alpha3$  ( $p = 0.001$ ) and a decrease in  $\alpha2$  ( $p = 0.0001$ ). This control analysis was performed because the change of only one frequency could have been incidental.

Of note, no differences were found neither for  $\beta1$ ,  $\beta2$ ,  $\gamma$  and  $\theta$  EEG power, nor  $\theta/\gamma$  frequency power ratio (all  $p > 0.11$ ). Although the mean perfusion in all the selected ROIs was similar between groups (all  $p > 0.38$ ), in the group with high  $\alpha3/\alpha2$  frequency ratio there was a constant trend toward a lower perfusion. Moreover, the left hippocampal volume was lower for AD-high risk patients when compared to the AD-low risk patients ( $p = 0.001$ ).

In patients at low risk for developing AD, significant Pearson's  $r$  negative correlation was found between perfusion in the hippocampal complex ROI and  $\theta$  rhythm ( $r = -0.544$ ,  $p = 0.044$ ).

In patients at high risk for developing AD otherwise, more dissimilar correlations were found: a positive correlation, inverted with respect to patients at low risk, between the perfusion in the hippocampal complex ROI and  $\theta$  rhythm ( $r = 0.729$ ,  $p = 0.005$ ), while temporal ROI correlated positively with  $\theta/\gamma$  ratio rhythms ( $r = 0.736$ ,  $p = 0.004$ ). No other significant correlations were found in both groups between perfusion ROIs and other EEG rhythms or hippocampal volumes. Moreover, no significant correlations were found between hippocampal complex ROI and  $\theta$  rhythm when pooling low and high risk patients together ( $r = 0.086$ ,  $p = 0.671$ ).

### Correlations between neuropsychological memory tests and regional brain perfusion in the high $\alpha3/\alpha2$ group and the other groups

*Babcock test:* a significant positive correlation was found in the high  $\alpha3/\alpha2$  group between logical memory performance on the Babcock test and lower perfusion values in bilateral precuneus ( $0.63$ ,  $p = 0.03$ ) and cortex in the

superior temporal sulcus ( $r = 0.74$ ,  $p = 0.005$ ). Moreover, a positive correlation was also found with hippocampal atrophy ( $r = 0.75$ ,  $p = 0.001$ ).

*AVLT immediate recall:* in the high  $\alpha3/\alpha2$  group memory performance significantly correlated with lower perfusion values in the caudal bank of the right inferior temporal sulcus and the middle frontal gyrus ( $r = 0.75$ ,  $p = 0.003$ ).

*AVLT delayed recall:* in the high  $\alpha3/\alpha2$  group memory function correlated significantly with lower perfusion values in the inferior parietal lobule, in particular in the supramarginal gyrus ( $r = 0.09$ ,  $p = 0.05$ ).

## Discussion

### Association between EEG markers and CGM changes

In the present study, the relationship between an EEG marker (the  $\alpha3/\alpha2$  power ratio) and the cortical thickness in subjects with MCI was investigated. The  $\alpha3/\alpha2$  power ratio has been chosen because in previous works it has been demonstrated that MCI subjects with higher  $\alpha3/\alpha2$  ratio are at major risk for developing AD [19-22]. Our results show that the MCI group with the higher  $\alpha3/\alpha2$  ratio has a greater global cortical atrophy than the other subgroups, thus confirming the claims of a large body of literature [6, 19]. Furthermore, greater atrophy is significant in two specific brain areas: precuneus and supramarginal gyrus (a brain area belonging to the inferior parietal lobule), both in the left and right hemispheres. These results were largely expected, considering the results of previous studies. Indeed, structural and functional abnormalities of the precuneus were observed in MCI [61-63] as well as in AD [64-66], so that the atrophy of the precuneal region has been considered as a pathognomonic marker of early AD. Recent studies suggest that specific regions, namely the precuneus and posterior cingulate, together with the medial temporal lobe, are selectively vulnerable to early amyloid deposition in AD pathology [67,68].

### Association between EEG markers and perfusional changes

These results confirm previous studies, which have shown that patients at high risk for

developing AD have reduced SPECT perfusion in the temporoparietal carrefour and inferior parietal lobule [55,56]. Moreover, our results also confirm a well-known correlation with hippocampal atrophy [55]. The present study shows a correlation between cerebral perfusion and  $\theta$  rhythm. The correlation emerges only when considering the different groups individuated on the  $\alpha3/\alpha2$  frequency power ratio. This is confirmed by the finding that when the groups are merged, no correlation could be found. This is the main aspect of the study and the peculiar novelty of the results. The patients at lower risk for developing AD, who have a constant trend towards a higher brain regional blood perfusion, maintain low levels of hippocampal  $\theta$  power while in patients at a higher risk, with a basically lower cerebral blood perfusion,  $\theta$  rhythm tends to be higher. Theta rhythms are usually not appreciated in a normal awakening EEG. However, a  $\theta$  power increase is observed over the frontal and temporal areas during learning and memory tasks. The  $\theta$  rhythms that are recorded during these tasks are thought to be produced by the activation of the septohippocampal system. The hippocampus has a cholinergic innervation originating from the basal forebrain, the medial septum, and the vertical limb of the diagonal band of Broca. Populations of GABAergic and glutamatergic neurons have also been described in several basal forebrain structures. The synchronized depolarization of hippocampal neurons produces field potentials that have a main frequency of 3-12 Hz and are usually known as hippocampal  $\theta$  rhythm [47,48]. The cholinergic-glutamatergic hypothesis of AD, in which most symptoms may be explained by cholinergic-glutamatergic deficits, has been advanced. Neuronal injury/loss may include an excitotoxic component that possibly contributes to the early cholinergic deficit. This excitotoxic component may occur, at least in part, at the septal level where the somas of cholinergic neurons reside. This insult may modify septal networks and contribute to the abnormal information processing observed in the AD brain, including its hyperexcitability states.

### Neurophysiological and clinical implications

Recent studies have demonstrated that there is a desynchronization in the temporoparietal memory-related networks during the successful encoding of new items, whereas synchronization prevents successful semantic encoding [66,69]. The deleterious role of synchronization has been recently demonstrated by an interesting study facing the intriguing relationship between functional and structural degeneration in AD [67]. These authors detected some hub regions (heteromodal associative regions) selectively vulnerable to AD pathology, due to the damage of inhibitory interneurons providing a loss of inhibition at the cellular level. According to the findings of these authors, the disinhibition provokes an increasing amount of neural activity at the network level, resulting in a hypersynchronization. A loss of inhibition also leads to alterations in calcium homeostasis and excitotoxicity [70,71]. Palop and Mucke also emphasize the role of inhibitory interneuron dysfunction, leading to hypersynchronization [72]. Our results are in line with these previous influential studies. A possible integrative view of all the results could be as follows: 1) the higher neuronal activity in the hub regions starts from a dysfunction of cellular inhibition; 2) the consequent disinhibition drives the neural network to an oversynchronization; 3) this over-synchronization is peculiar in the hub regions with higher amyloid burden; 4) these over-activated regions are prone to degeneration and atrophy; 5) a possible neurophysiologic sign of this oversynchronization is the increase of the  $\alpha3/\alpha2$  power ratio we have found in typical hub regions [73-77]. It is of great interest that there is an overlap between the brain regions associated with the increase in EEG  $\alpha3/\alpha2$  power ratio (hypersynchronization of the upper  $\alpha$ ) in our study and the regions associated with a higher amyloid burden related to memory processes [70, 71]. Moreover, in the present study, there is a very interesting finding: the atrophy of the precuneus is coupled with the atrophy of the supramarginal gyrus and, to a lesser extent, with the inferior parietal lobule, insula and superior temporal gyrus.

This atrophy pattern is clearly expressed in the group of MCI subjects with higher  $\alpha3/\alpha2$  power ratio. This finding fits well with the results of a recent study [78], which investigated the functional connectivity of human precuneus by resting state fMRI. The authors found that there is a preferential pathway of connectivity of the dorsal precuneus with the supramarginal gyrus, parietal cortex, superior temporal gyrus and insula. As a consequence, the atrophy we detected in the MCI group with higher  $\alpha3/\alpha2$  ratio power could be explained as the loss of GM in an entire anatomo-functional network rather than atrophy of isolated brain areas. Of note, it is widely accepted that AD is the result of cortical network impairment more than the atrophy of single cortical areas [79]. In subjects with low or middle  $\alpha3/\alpha2$  power ratio, the cognitive impairment is possibly due to cerebrovascular impairment or non-AD degenerative process. Although the rigid selection criteria were adopted to include patients with primary cognitive deficits in the study, in clinical practice it is not infrequent to have MCI subjects due to reasons other than AD.

### Memory performance

In order to exclude a random relationship between EEG marker and cortical atrophy, the correlation between brain areas and the performance on memory tests was investigated in all MCI subgroups. The memory tests used were selected due to their well-known sensitivity to detect MCI subjects who will convert to AD [1,9]. Our results show no significant memory differences between the groups studied. This could be considered as a paradoxical outcome. However, we think this should not be taken as a surprise, having in mind the globally mild and early impairment of the whole group of subjects. In other words, when considering strictly the memory performance, the groups are not different. This is probably due to early, and generally mild, cognitive impairment. Despite no significant difference in memory test scores, when focusing on the relationship between the memory performance and a reliable structural marker such as the cortical thickness, the MCI group with the higher  $\alpha3/\alpha2$  power ratio has shown

a (negative) correlation between memory test performance and cortical thickness, as expected in patients with probable prodromal AD. This result confirms the peculiar nature of this MCI group, showing a clear specificity with regards to both the cortical atrophy and the correlated memory performance. Moreover, no other socio-demographical or structural differences were observed in the MCI groups that could explain the correlation analysis results. The cortical areas associated with cortical thinning and those correlated with memory test performance are only partly overlapping. This could be due to the particular nature of the memory domain, underpinning a large number of brain areas. On the other hand, MCI subjects more susceptible to converting to AD could also show impairment in other cognitive domains, such as visuospatial attention or in execution and preparation of spatially guided behavior [80-83]. Of note, the cortical network encompassing precuneus and inferior parietal cortex is deeply involved in visuospatial abilities [78]. As a speculative interpretation, we could hypothesize that the memory deficits could be due to an impaired network underlying the semantic coding of the spatial features of the episodic memory traces. In this view, the atrophy of a specific brain network (more than global volume measures) is more reliable in detecting MCI subjects with prodromal AD. Further discussion of memory-related brain networks is beyond the scope of this study. Only a weak negative correlation was found in the middle  $\alpha3/\alpha2$  EEG power ratio, suggesting a possible degenerative nature of the memory impairment in this group. Significant associations were not identified in the low  $\alpha3/\alpha2$  power ratio group or in the study sample as a whole. Taken together, these results strengthen the position of the higher  $\alpha3/\alpha2$  ratio in MCI group of subjects as a major risk factor for developing AD.

### Alterations of functional coupling of temporoparietal areas

Linear EEG coherence is a reliable measure of the functional coupling of brain areas. The present study demonstrates that MCI subjects show a general decrease of coherence except for an increase of interhemispheric coherence

in temporoparietal regions, especially in  $\theta$  frequency. A previous study has demonstrated that this increase is due to hippocampal atrophy [18].

Previous studies showed that the increase of coherence between temporal regions is determined by an increase in excitability [84-88]. This hypothesis could receive support from studies demonstrating a dysregulation of inhibitory GABAergic system following the hippocampal atrophy [88-91]. Through the hippocampal commissure, the increase in excitability could spread over the two hemispheres. It could be explained as a compensatory mechanism, since it is more frequently observed in subjects with hippocampal atrophy. Moreover, it could be argued that this activity emerges as the new default mode of brain activity characterized by a hyperexcitability of the cortex, even in a resting state.

### Implications at system level

Klimesch and coworkers have convincingly demonstrated that the upper  $\alpha$  band (~10-13 Hz) specifically reflects processes necessary for memory encoding [84,85]. Recent EEG and magnetoencephalography (MEG) studies have confirmed that proper functioning of memory, both in encoding and in retrieval, requires high  $\alpha$  rhythm desynchronization (or power decrease) [24,86-91]. From a neurophysiological point of view, the synchronization (or power increase) of EEG  $\alpha$  power has been associated with the inhibition timing hypothesis [24] and with poor information transmission, according to the entropy's theory [27,92]. The increases in  $\alpha$  amplitudes reflect inhibition of cortical

brain regions [25,26,93]. Similarly, the theory of entropy states that synchronization is disadvantageous for storing information, as it reduces the flow of information [27]. Entropy is a measure of the richness of information encoded in a sequence of events. Applying this concept to neural networks, it has been demonstrated [78] that the degree of information that is encoded in neural assemblies increases as a function of desynchronization and decreases as a function of synchronized firing patterns [94, 95]. This hypothesis has been confirmed in clinical studies in patients with memory deficits [96], as well as during states where there is little cognitive processing (e.g., epileptic seizures or slow-wave sleep) [78,97,98]. With regards to the cognitive impairment due to AD, the typical synaptic loss could prevent the physiological flexibility of brain neural assemblies, impeding the desynchronizing downstream modulation of brain activity. As a consequence, it could be hypothesized that the disruption of the cortical network due to degenerative disease, inducing cortical atrophy, could cause an oversynchronization of the brain oscillatory activity. The synchronization state of the high  $\alpha$  power could prevent the creation of a semantic sensory code and, consequently, of the episodic memory trace [99-101]. In previous seminal studies, high  $\alpha$  frequency has been specifically related to semantic memory processes [41, 102]. Of note, in subjects with early cognitive decline, the impairment of the semantic features of memory has been recently accepted as a hallmark for the early diagnosis of AD [1, 2]. Indeed, according to the new diagnostic criteria of AD, the measurement of sensitivity to semantic cueing can be used to successfully

differentiate patients with AD from healthy controls, even when patients are almost equal to controls on MMSE scores or when disease severity is very mild. Our results are generally in line with this hypothesis, suggesting that an increase in the power of high  $\alpha$  brain oscillations reflects a block of information processing. However, the present study goes one step further, linking the increase of high  $\alpha$  synchronization to the atrophy of a specific brain network, correlated with impairment in memory performance. Moreover, according to this theory, the increased  $\theta$  production in AD would derive from hyperexcitability of the septohippocampal system [15,16,103-117]. Such a pattern of decreased cerebral blood flow activity and increased excitability was found even prior to the onset of cognitive impairment and cortical atrophy [17, 18].

### Conclusion

A high EEG upper/low  $\alpha$  power ratio was associated with cortical thinning and lower perfusion in the temporoparietal area. In these subjects an increase in the production of  $\theta$  oscillations has been observed associated with a greater interhemispheric coupling between temporal areas. Moreover, atrophy and lower perfusion rate both significantly correlated with memory impairment in MCI subjects.

### Acknowledgment

*Conflict of interest statement:* The author declares that he has no actual or potential conflicts of interest.

### References

- [1] Dubois B, Feldman H.H., Jacova C., DeKosky S.T., Barberger-Gateau P, Cummings J, et al., Research criteria for the diagnosis of Alzheimer's disease: revising the NINCDS-ADRDA criteria, *Lancet Neurol.*, 2007, 6, 734-746
- [2] Albert M.S., DeKosky S.T., Dickson D., Dubois B., Feldman H.H., Fox N.C., et al., The diagnosis of mild cognitive impairment due to Alzheimer's disease: recommendations from the National Institute on Aging - Alzheimer's Association workgroups on diagnostic guidelines for Alzheimer's disease, *Alzheimers Dement.*, 2011, 7, 270-279
- [3] Hampel H., Bürger K., Teipel S.J., Bokde A.L., Zetterberg H., Blennow K., Core candidate neurochemical and imaging biomarkers of Alzheimer's disease, *Alzheimers Dement.*, 2008, 4, 38-48
- [4] Galluzzi S., Geroldi C., Amicucci G., Bocchio-Chiavetto L., Bonetti M., Bonvicini C., et al., Supporting evidence for using biomarkers in the diagnosis of MCI due to AD, *J. Neurol.*, 2013, 260, 640-650
- [5] Frisoni G.B., Sabattoli F., Lee A.D., Dutton R.A., Toga A.W., Thompson P.M., In vivo neuropathology of the hippocampal formation in AD: a radial mapping MR-based study. *Neuroimage*, 2006, 32, 104-110
- [6] Frisoni G.B., Pievani M., Testa C., Sabattoli F., Bresciani L., Bonetti M., et al., The topography of grey matter involvement in early and late onset Alzheimer's disease, *Brain*, 2007, 130, 720-730

- [7] Frisoni G.B., Ganzola R., Canu E., Rüb U., Pizzini F.B., Alessandrini F., et al., Mapping local hippocampal changes in Alzheimer's disease and normal ageing with MRI at 3 Tesla, *Brain*, 2008, 131, 3266-3276
- [8] Frisoni G.B., Prestia A., Rasser P.E., Bonetti M., Thompson P.M., In vivo mapping of incremental cortical atrophy from incipient to overt Alzheimer's disease, *J. Neurol.*, 2009, 256, 916-924
- [9] Frisoni G.B., Alzheimer disease: biomarker trajectories across stages of Alzheimer disease, *Nat. Rev. Neurol.*, 2012, 8, 299-300
- [10] van Strien N.M., Cappaert N.L., Witter M.P., The anatomy of memory: an interactive overview of the parahippocampal-hippocampal network, *Nat. Rev. Neurosci.*, 2009, 10, 272-282
- [11] Missonnier P., Herrmann F.R., Michon A., Fazio-Costa L., Gold G., Giannakopoulos P., Early disturbances of gamma band dynamics in mild cognitive impairment, *J. Neural Transm.*, 2010, 117, 489-498
- [12] Steriade M., Grouping of brain rhythms in corticothalamic systems, *Neuroscience*, 2006, 137, 1087-1106
- [13] Hogan M.J., Swanwick G.R.J., Kaiser J., Rowan M., Lawlor B., Memory-related EEG power and coherence reductions in mild Alzheimer's disease, *Int. J. Psychophysiol.*, 2003, 43, 147-163
- [14] Lopes da Silva F.H., Vos J.E., Mooibroek J., van Rotterdam A., Relative contributions of intracortical and thalamo-cortical processes in the generation of alpha rhythms, revealed by partial coherence analysis, *Electroencephalogr. Clin. Neurophysiol.*, 1980, 50, 449-456
- [15] Ingber L., Nunez P.L., Neocortical dynamics at multiple scales: EEG standing waves, statistical mechanics, and physical analogs, *Math. Biosci.*, 2011, 229, 160-173
- [16] Nunez P.L., Generation of human EEG rhythms by a combination of long and short-range neocortical interactions, *Brain Topogr.*, 1989, 1, 199-215
- [17] Stam C.J., Montez T., Jones B.F., Rombouts S.A., van der Made Y., Pijnenburg Y.A., et al., Disturbed fluctuations of resting state EEG synchronization in Alzheimer's disease, *Clin. Neurophysiol.*, 2005, 116, 708-715
- [18] Moretti D.V., Miniussi C., Frisoni G.B., Geroldi C., Zanetti O., Binetti G., et al., Hippocampal atrophy and EEG markers in subjects with mild cognitive impairment, *Clin. Neurophysiol.*, 2007, 118, 2716-2729
- [19] Moretti D.V., Pievani M., Fracassi C., Binetti G., Rosini S., Geroldi C., et al., Increase of theta/gamma and alpha3/alpha2 ratio is associated with amygdalo-hippocampal complex atrophy, *J. Alzheimers Dis.*, 2009, 17, 349-357
- [20] Moretti D.V., Frisoni G.B., Pievani M., Rosini S., Geroldi C., Binetti G., et al., Cerebrovascular disease and hippocampal atrophy are differently linked to functional coupling of brain areas: an EEG coherence study in MCI subjects, *J. Alzheimers Dis.*, 2008, 14, 285-299
- [21] Moretti D.V., Babiloni C., Binetti G., Cassetta E., Dal Forno G., Ferreri F., et al., Individual analysis of EEG frequency and band power in mild Alzheimer's disease, *Clin. Neurophysiol.*, 2004, 115, 299-308
- [22] Moretti D.V., Miniussi C., Frisoni G., Zanetti O., Binetti G., Geroldi C., et al., Vascular damage and EEG markers in subjects with mild cognitive impairment, *Clin. Neurophysiol.*, 2007, 118, 1866-1876
- [23] Moretti D.V., Frisoni G.B., Pievani M., Fracassi C., Geroldi C., Calabria M., et al., Brain vascular damage of cholinergic pathways and EEG markers in mild cognitive impairment, *J. Alzheimers Dis.*, 2008, 15, 357-372
- [24] Bakkour A., Morris J.C., Dickerson B.C., The cortical signature of prodromal AD: regional thinning predicts mild AD dementia, *Neurology*, 2009, 72, 1048-1055
- [25] Klimesch W., Doppelmayr M., Hanslmayr S., Upper alpha ERD and absolute power: their meaning for memory performance, *Prog. Brain Res.*, 2006, 159, 151-165
- [26] Klimesch W., Sauseng P., Hanslmayr S., EEG alpha oscillations: the inhibition timing hypothesis, *Brain Res. Rev.*, 2007, 53, 63-88
- [27] Klimesch W., Evoked alpha and early access to the knowledge system: the P1 inhibition timing hypothesis, *Brain Res.*, 2011, 1408, 52-71
- [28] Folstein M.F., Folstein S.E., McHugh P.R., "Mini-mental state": A practical method for grading the cognitive state of patients for clinician, *J. Psychiatr. Res.*, 1975, 12, 189-198
- [29] Hughes C.P., Berg L., Danziger W.L., Cohen L.A., Martin R.L., A new clinical rating scale for the staging of dementia, *Br. J. Psychiatry*, 1982, 140, 1225-1230
- [30] Rosen W.G., Terry R.D., Fuld P.A., Katzman R., Peck A., Pathological verification of ischemic score in differentiation of dementias, *Ann. Neurol.*, 1980, 7, 486-488
- [31] Lawton M.P., Brodie E.M., Assessment of older people: self-maintaining and instrumental activity of daily living, *Gerontologist*, 1969, 9, 179-186
- [32] Petersen R.C., Doody R., Kurz A., Mohs R.C., Morris J.C., Rabins P.V., et al., Current concepts in mild cognitive impairment, *Arch. Neurol.*, 2001, 58, 1985-1992
- [33] Portet F., Ousset P.J., Visser P.J., Frisoni G.B., Nobili F., Scheltens P., et al., Mild cognitive impairment (MCI) in medical practice: a critical review of the concept and new diagnostic procedure. Report of the MCI Working Group of the European Consortium on Alzheimer's Disease, *J. Neurol. Neurosurg. Psychiatry*, 2006, 77, 714-718
- [34] Lezak M., Howieson D., Loring D.W., *Neuropsychological assessment*, Fourth edition, Oxford University Press, Oxford, UK, 2004
- [35] Radloff L.S., The CES-D scale: a self-report depression scale for research in the general population, *Appl. Psychol. Measure.*, 1977, 1, 385-401
- [36] Kaplan A.Y., The problem of segmental description of human electroencephalogram, *Hum. Physiol.*, 1999, 25, 107-114
- [37] Cohen B.A., Sances A.Jr., Stationarity of the human electroencephalogram, *Med. Biol. Eng. Comput.*, 1977, 15, 513-518
- [38] Kawabata N., Test of statistical stability of the electroencephalogram, *Biol. Cybern.*, 1976, 22, 235-238
- [39] McEwen J.A., Anderson G.B., Modeling the stationarity and gaussianity of spontaneous electroencephalographic activity, *IEEE Trans. Biomed. Eng.*, 1975, 22, 361-369
- [40] Kipiński L., König R., Sielużycki C., Kordecki W., Application of modern tests for stationarity to single-trial MEG data: transferring powerful statistical tools from econometrics to neuroscience, *Biol. Cybern.*, 2011, 105, 183-195
- [41] Moretti D.V., Fracassi C., Pievani M., Geroldi C., Binetti G., Zanetti O., et al., Increase of theta/gamma ratio is associated with memory impairment, *Clin. Neurophysiol.*, 2009, 120, 295-303

- [42] Moretti D.V., Pievani M., Fracassi C., Binetti G., Rosini S., Geroldi C., et al., Increase of theta/gamma and alpha3/alpha2 ratio is associated with amygdalo-hippocampal complex atrophy, *J. Alzheimers Dis.*, 2009, 17, 349-357
- [43] Moretti D.V., Pievani M., Geroldi C., Binetti G., Zanetti O., Cotelli M., et al., Increasing of hippocampal atrophy and cerebrovascular damage is differently associated with functional cortical coupling in MCI patients, *Alzheimer Dis. Assoc. Disord.*, 2009, 23, 323-332
- [44] Cabeza R., Hemispheric asymmetry reduction in older adults: the HAROLD model, *Psychol. Aging*, 2002, 17, 85-100
- [45] Balsters J.H., O'Connell R.G., Galli A., Nolan H., Greco E., Kilcullen S.M., et al., Changes in resting connectivity with age: a simultaneous electroencephalogram and functional magnetic resonance imaging investigation, *Neurobiol. Aging*, 2013, 34, 2194-2207
- [46] Watson P., Conroy A., Moran G., Duncan S., Retrospective study of sensitivity and specificity of EEG in the elderly compared with younger age groups, *Epilepsy Behav.*, 2012, 25, 408-411
- [47] Tenke C.E., Kayser J., Miller L., Warner V., Wickramaratne P., Weissman M.M., et al., Neuronal generators of posterior EEG alpha reflect individual differences in prioritizing personal spirituality, *Biol. Psychol.*, 2013, 94, 426-432
- [48] Grandy T.H., Werkle-Bergner M., Chicherio C., Schmiedek F., Lövdén M., Lindenberger U., Peak individual alpha frequency qualifies as a stable neurophysiological trait marker in healthy younger and older adults, *Psychophysiology*, 2013, 50, 570-582
- [49] Grandy T.H., Werkle-Bergner M., Chicherio C., Lövdén M., Schmiedek F., Lindenberger U., Individual alpha peak frequency is related to latent factors of general cognitive abilities, *Neuroimage*, 2013, 79, 10-18
- [50] Bekhtereva V., Sander C., Forschack N., Olbrich S., Hegerl U., Müller M.M., Effects of EEG-vigilance regulation patterns on early perceptual processes in human visual cortex, *Clin. Neurophysiol.*, 2014, 125, 98-107
- [51] Ségonne F., Dale A.M., Busa E., Glessner M., Salat D., Hahn H.K., et al., A hybrid approach to the skull stripping problem in MRI, *Neuroimage*, 2004, 22, 1060-1075
- [52] Fischl B., Dale A.M., Measuring the thickness of the human cerebral cortex using magnetic resonance images, *Proc. Natl. Acad. Sci. USA*, 2000, 97, 11044-11049
- [53] Han X., Jovicich J., Salat D., van der Kouwe A., Quinn B., Czanner S., et al., Reliability of MRI-derived measurements of human cerebral cortical thickness: the effects of field strength, scanner upgrade and manufacturer, *Neuroimage*, 2006, 32, 180-194
- [54] Gronenschild E.H., Habets P., Jacobs H.I., Mengelers R., Rozendaal N., van Os J., et al., The effects of FreeSurfer version, workstation type, and Macintosh operating system version on anatomical volume and cortical thickness measurements, *PLoS One*, 2012, 7, 238-234
- [55] DeCarli C., Fletcher E., Ramey V., Harvey D., Jagust W.J., Anatomical mapping of white matter hyperintensities (WMH): exploring the relationships between periventricular WMH, deep WMH, and total WMH burden, *Stroke*, 2005, 36, 50-55
- [56] Pennanen C., Testa C., Laasko M.P., Hallikainen M., Helkala E.L., Hanninen T., et al., A voxel based morphometry study on mild cognitive impairment, *J. Neurol. Neurosurg. Psychiatry*, 2005, 76, 11-14
- [57] Markesbery W.R., Schmitt R.A., Kryscio R.J., Davis D., Smith C., Wekstein D. Neuropathologic substrate of mild cognitive impairment, *Arch. Neurol.*, 2006, 63, 38-46
- [58] McKhann G.M., Knopman D.S., Chertkow H., Hyman B.T., Jack C.R.Jr, Kawas C.H., et al., The diagnosis of dementia due to Alzheimer's disease: recommendations from the national institute on aging-Alzheimer's association workgroups on diagnostic guidelines for Alzheimer's disease, *Alzheimers Dement.*, 2011, 7, 263-269
- [59] Sperling R.A., Aisen P.S., Beckett L.A., Bennett D.A., Craft S., Fagan A.M., et al., Toward defining the preclinical stages of Alzheimer's disease: recommendations from the National Institute on Aging-Alzheimer's Association workgroups on diagnostic guidelines for Alzheimer's disease, *Alzheimers Dement.*, 2011, 7, 280-292
- [60] Caroli A., Testa C., Geroldi C., Nobili F., Guerra U.P., Bonetti M., et al., Brain perfusion correlates of medial temporal lobe atrophy and white matter hyperintensities in mild cognitive impairment, *J. Neurol.*, 2007, 254, 1000-1008
- [61] Matsuda H., The role of neuroimaging in mild cognitive impairment, *Neuropathology*, 2007, 27, 570-577
- [62] Petrella J.R., Wang L., Krishnan S., Slavin M.J., Prince S.E., Tran T.T., et al., Cortical deactivation in mild cognitive impairment: high-field-strength functional MR imaging, *Radiology*, 2007, 245, 224-235
- [63] Pihlajamaki M., Jauhiainen A.M., Soininen H., Structural and functional MRI in mild cognitive impairment, *Curr. Alzheimer Res.*, 2009, 6, 179-185
- [64] Dickerson B.C., Sperling R.A., Large-scale functional brain network abnormalities in Alzheimer's disease: insights from functional neuroimaging, *Behav. Neurol.*, 2009, 21, 63-75
- [65] Ryu S.Y., Kwon M.J., Lee S.B., Yang D.W., Kim T.W., Song I.U., et al., Measurement of precuneal and hippocampal volumes using magnetic resonance volumetry in Alzheimer's disease, *J. Clin. Neurol.*, 2010, 6, 196-203
- [66] Sperling R.A., Dickerson B.C., Pihlajamaki M., Vannini P., LaViolette P.S., Vitolo O.V., et al., Functional alterations in memory networks in early Alzheimer's disease, *Neuromolecular Med.*, 2010, 12, 27-43
- [67] de Haan W., Mott K., van Straaten E.C., Scheltens P., Stam C.J., Activity dependent degeneration explains hub vulnerability in Alzheimer's disease, *PLoS Comput. Biol.*, 2012, 8, e1002582
- [68] Pievani M., de Haan W., Wu T., Seeley W.W., Frisoni G.B., Functional network disruption in the degenerative dementias, *Lancet Neurol.*, 2011, 10, 829-843
- [69] Chatwal J.P., Sperling R.A., Functional MRI of mnemonic networks across the spectrum of normal aging, mild cognitive impairment, and Alzheimer's disease, *J. Alzheimers Dis.*, 2012, 31, S155-167
- [70] Jones D.T., Machulda M.M., Vemuri P., McDade E.M., Zeng G., Senjem M.L., et al., Age-related changes in the default mode network are more advanced in Alzheimer disease, *Neurology*, 2011, 77, 1524-1531
- [71] Brier M.R., Thomas J.B., Snyder A.Z., Benzinger T.L., Zhang D., Raichle M.E., et al., Loss of intranetwork and internetwork resting state functional connections with Alzheimer's disease progression, *J. Neurosci.*, 2012, 32, 8890-8899



- [72] Palop J.J., Mucke L., Synaptic depression and aberrant excitatory network activity in Alzheimer's disease: two faces of the same coin?, *Neuromolecular Med.*, 2010, 12, 48-55
- [73] Stam C.J., van der Made Y., Pijnenburg Y.A., Scheltens P., EEG synchronization in mild cognitive impairment and Alzheimer's disease, *Acta Neurol. Scand.*, 2003, 108, 90-96
- [74] Bhattacharya B.S., Coyle D., Maguire L.P., Alpha and theta rhythm abnormality in Alzheimer's disease: a study using a computational model, *Adv. Exp. Med. Biol.*, 2011, 718, 57-73
- [75] Rossini P.M., Buscema M., Capriotti M., Grossi E., Rodriguez G., Del Percio C., et al., Is it possible to automatically distinguish resting EEG data of normal elderly vs. mild cognitive impairment subjects with high degree of accuracy?, *Clin. Neurophysiol.*, 2008, 119, 1534-1545
- [76] Wu X., Li R., Fleisher A.S., Reiman E.M., Guan X., Zhang Y., et al., Altered default mode network connectivity in Alzheimer's disease - a resting functional MRI and Bayesian network study, *Hum. Brain Mapp.*, 2011, 32, 1868-1881
- [77] Wonderlick J.S., Ziegler D.A., Hosseini-Varnamkhasti P., Locascio J.J., Bakkour A., van der Kouwe A., et al., Reliability of MRI-derived cortical and subcortical morphometric measures: effects of pulse sequence, voxel geometry, and parallel imaging, *Neuroimage*, 2009, 44, 1324-1333
- [78] Zhang S., Li C.S., Functional connectivity mapping of the human precuneus by resting state fMRI, *Neuroimage*, 2012, 59, 3548-3562
- [79] Morbelli S., Drzezga A., Perneczky R., Frisoni G.B., Caroli A., van Berckel B.N., et al., Resting metabolic connectivity in prodromal Alzheimer's disease. A European Alzheimer Disease Consortium (EADC) project, *Neurobiol. Aging*, 2012, 33, 2533-2550
- [80] Ghaem O., Mellet E., Crivello F., Tzourio N., Mazoyer B., Berthoz A., et al., Mental navigation along memorized routes activates the hippocampus, precuneus, and insula, *Neuroreport*, 1997, 8, 739-744
- [81] Leichnetz G.R., Connections of the medial posterior parietal cortex (area 7m) in the monkey, *Anat. Rec.*, 2001, 263, 215-236
- [82] Cavanna A.E., Trimble M.R., The precuneus: a review of its functional anatomy and behavioural correlates, *Brain*, 2006, 129, 564-583
- [83] Wenderoth N., Debaere F., Snaert S., Swinnen S.P., The role of anterior cingulate cortex and precuneus in the coordination of motor behaviour, *Eur. J. Neurosci.*, 2005, 22, 235-246
- [84] Klimesch W., Schimke H., Doppelmayr M., Ripper B., Schwaiger J., Pfurtscheller G., Event-related desynchronization (ERD) and the Dm effect: does alpha desynchronization during encoding predict late recall performance?, *Int. J. Psychophysiol.*, 1996, 24, 47-60
- [85] Klimesch W., Doppelmayr M., Stadler W., Pöllhuber D., Sauseng P., Röhms D., Episodic retrieval is reflected by a process specific increase in human electroencephalographic theta activity, *Neurosci. Lett.*, 2001, 302, 49-52
- [86] Fries P., Reynolds J.H., Rorie A.E., Desimone R., Modulation of oscillatory neuronal synchronization by selective visual attention, *Science*, 2001, 291, 1560-1563
- [87] Kilner J.M., Mattout J., Henson R., Friston K.J., Hemodynamic correlates of EEG: a heuristic, *Neuroimage*, 2005, 28, 280-286
- [88] Wyart V., Tallon-Baudry C., Neural dissociation between visual awareness and spatial attention, *J. Neurosci.*, 2008, 28, 2667-2679
- [89] Spitzer B., Hanslmayr S., Opitz B., Mecklinger A., Bäuml K.-H., Oscillatory correlates of retrieval-induced forgetting in recognition memory, *J. Cogn. Neurosci.*, 2009, 21, 976-990
- [90] Staudigl T., Hanslmayr S., Bäuml K.-H., Theta oscillations reflect the dynamics of interference in episodic memory retrieval, *J. Neurosci.*, 2010, 30, 11356-11362
- [91] Hanslmayr S., Staudigl T., Aslan A., Bäuml K.-H., Theta oscillations predict the detrimental effects of memory retrieval, *Cogn. Affect. Behav. Neurosci.*, 2010, 10, 329-338
- [92] Hanslmayr S., Staudigl T., Fellner M.C., Oscillatory power decreases and long-term memory: the information via desynchronization hypothesis, *Front. Hum. Neurosci.*, 2012, 6, 74
- [93] Jensen O., Mazaheri A., Shaping functional architecture by oscillatory alpha activity: gating by inhibition, *Front. Hum. Neurosci.*, 2010, 4, 186
- [94] Norman K.A., How hippocampus and cortex contribute to recognition memory: revisiting the complementary learning systems model, *Hippocampus*, 2010, 20, 1217-1227
- [95] Schneidman E., Puchalla J.L., Segev R., Harris R.A., Bialek W., Berry M.J., Synergy from silence in a combinatorial neural code, *J. Neurosci.*, 2011, 31, 15732-15741
- [96] Kurimoto R., Ishii R., Canuet L., Ikezawa K., Iwase M., Azechi M., et al., Induced oscillatory responses during the Sternberg's visual memory task in patients with Alzheimer's disease and mild cognitive impairment, *Neuroimage*, 2012, 59, 4132-4140
- [97] Goard M., Dan Y., Basal forebrain activation enhances cortical coding of natural scenes, *Nat. Neurosci.*, 2009, 12, 1444-1449
- [98] Chalk M., Herrero J.L., Gieselmann M.A., Delicato L.S., Gotthardt S., Thiele A., Attention reduces stimulus-driven gamma frequency oscillations and spike field coherence in V1, *Neuron*, 2010, 66, 114-125
- [99] Barlow H.B., The coding of sensory messages, In: *Current problems in animal behaviour*, Eds. Thorpe W.H., Zangwill O.L., Cambridge University Press, Cambridge, UK, 1961, 331-360
- [100] Bialek W., Rieke F., de Ruytervan Steveninck R.R., Warland D., Reading a neural code, *Science*, 1991, 252, 1854-1857
- [101] Hanslmayr S., Spitzer B., Bäuml K.-H., Brain oscillations dissociate between semantic and non semantic encoding of episodic memories, *Cereb. Cortex*, 2009, 19, 1631-1640
- [102] Craik F.I.M., Levels of processing: past, present and future?, *Memory*, 2002, 10, 305-318
- [103] Moretti D.V., Pievani M., Geroldi C., Binetti G., Zanetti O., Rossini P.M., et al., EEG markers discriminate among different subgroup of patients with mild cognitive impairment, *Am. J. Alzheimers Dis. Other Demen.*, 2010, 25, 58-73
- [104] Moretti D.V., Frisoni G.B., Fracassi C., Pievani M., Geroldi C., Binetti G., et al., MCI patients' EEGs show group differences between those who progress and those who do not progress to AD, *Neurobiol. Aging*, 2011, 32, 563-571
- [105] Moretti D.V., Frisoni G.B., Binetti G., Zanetti O., Anatomical substrate and scalp EEG markers are correlated in subjects with cognitive impairment and Alzheimer's disease, *Front. Psychiatry*, 2011, 1, 152

- [106] Moretti D.V., Prestia A., Fracassi C., Geroldi C., Binetti G., Rossini P.M., et al., Volumetric differences in mapped hippocampal regions correlate with increase of high alpha rhythm in Alzheimer's disease, *Int. J. Alzheimers Dis.*, 2011, 208218
- [107] Moretti D.V., Paternicò D., Binetti G., Zanetti O., Frisoni G.B., EEG markers are associated to gray matter changes in thalamus and basal ganglia in subjects with mild cognitive impairment, *Neuroimage*, 2012, 60, 489-496
- [108] Moretti D.V., Prestia A., Fracassi C., Binetti G., Zanetti O., Frisoni G.B., Specific EEG changes associated with atrophy of hippocampus in subjects with mild cognitive impairment and Alzheimer's disease, *Int. J. Alzheimers Dis.*, 2012, 253153
- [109] Moretti D.V., Zanetti O., Binetti G., Frisoni G.B., Quantitative EEG markers in mild cognitive impairment: degenerative versus vascular brain impairment, *Int. J. Alzheimers Dis.*, 2012, 917537
- [110] Moretti D.V., Paternicò D., Binetti G., Zanetti O., Frisoni G.B., Analysis of grey matter in thalamus and basal ganglia based on EEG alpha3/alpha2 frequency ratio reveals specific changes in subjects with mild cognitive impairment, *ASN Neuro*, 2012, 4, e00103
- [111] Moretti D.V., Paternicò D., Binetti G., Zanetti O., Frisoni G.B., Relationship between EEG alpha3/alpha2 ratio and the nucleus accumbens in subjects with mild cognitive impairment, *J. Neurol. Neurophysiol.*, 2013, 4, 149
- [112] Moretti D.V., Paternicò D., Binetti G., Zanetti O., Frisoni G.B., Theta/gamma frequency ratio is associated to grey matter changes in basal ganglia in subjects with mild cognitive impairment, *J. Radiol. Diagn. Imaging*, 2013, 1, 10-18
- [113] Moretti D.V., Paternicò D., Binetti G., Zanetti O., Frisoni G.B., Temporo-parietal brain network impairment is related to EEG alpha3/alpha2 power ratio in prodromal Alzheimer's disease, *J. Neurol. Neurophysiol.*, 2013, 4, 160
- [114] Moretti D.V., Paternicò D., Binetti G., Zanetti O., Frisoni G.B., EEG upper/low alpha frequency power ratio relates to temporo-parietal brain atrophy and memory performances in mild cognitive impairment, *Front. Aging Neurosci.*, 2013, 5, 63
- [115] Moretti D.V., Prestia A., Binetti G., Zanetti O., Frisoni G.B., Increase of theta frequency is associated with reduction in regional cerebral blood flow only in subjects with mild cognitive impairment with higher upper alpha/low alpha EEG frequency power ratio, *Front. Behav. Neurosci.*, 2013, 7, 188
- [116] Moretti D.V., Prestia A., Binetti G., Zanetti O., Frisoni G.B., Correlation between regional cerebral blood flow and EEG upper/low alpha frequency power ratio in mild cognitive impairment, *J. Radiol. Diagn. Imaging*, 2013, 1, 49-59
- [117] Moretti D.V., Paternicò D., Binetti G., Zanetti O., Frisoni G.B., Electroencephalographic upper/low alpha frequency power ratio relates to cortex thinning in mild cognitive impairment, *Neurodegener. Dis.*, 2014, 14, 18-30